*2020 IEEE PES/IAS PowerAfrica*

# Thermal model and disturbance co-identification using optimization and filtering techniques

Heman Shamachurn
Department of Electrical and Electronic Engineering,
Faculty of Engineering,
University of Mauritius
Reduit, Mauritius
h.shamachurn@uom.ac.mu

S Z Sayed Hassen
Department of Electrical and Electronic Engineering,
Faculty of Engineering,
University of Mauritius
Reduit, Mauritius
z.sayedhassen@uom.ac.mu

***Abstract*— Buildings can participate in demand-side management through anticipatory control techniques. Model-based control methods offer promising avenues to improve the energy efficiency in the build environment. The required thermal model needs to have a low complexity while reproducing the dynamics accurately. Unmeasured heat sources occurring mainly due to occupancy affect the grey-box model identification. In this work, an optimization-based and a Kalman filter-based technique are compared for the simultaneous identification of both an RC grey-box thermal model and the associated disturbance using input-output data. It is found that while the filtering-based method is less computationally intensive, it can produce similar results as the optimization-based method. It was found that including constraints in the Kalman filter improves the estimated disturbance while noise and wide parameter bounds severely affect the performances of both techniques. Moreover, the initial state estimate does have an impact on the resulting estimation in both techniques.**

***Keywords— grey-box model, fmincon, extended kalman filter, disturbances, model identification***

## I. INTRODUCTION

In 2018, buildings were estimated to consume about 30 % of the global final energy use and this was associated with about 28 % of energy-related $CO_2$ emissions worldwide [1]. Heating, Ventilation and Air-Conditioning (HVAC) systems currently consume about 37 % of the total energy used by buildings [2]. Implementation of new or improvement of existing building energy management systems through advanced control technologies can greatly enhance the energy efficiency of existing building energy systems [3]. Inappropriate sensing and controls, and the inability to explore the full potential of existing building control systems case are responsible for about 30 % of energy wastage in commercial buildings [4]. The traditional systems such as ON/OFF and Proportional-Integral-Derivative (PID) controllers may not be as energy-efficient as the model-based predictive controllers [5], [6]. The latter can perform anticipatory control rather than corrective control, accounting for disturbance model to allow for disturbance rejection, handle constraints and uncertainties, and deal with time-varying system dynamics and various operating conditions [7].

Model-based control techniques require a model which can reproduce the thermal dynamics of the zone with an acceptable level of accuracy and minimal complexity. The model development stage is still the most time consuming and expensive part of a control approach such as a predictive-control implementation project [8], [9]. Model can be classified as white, grey and black-boxes. They can also be linear or non-linear as well as time-varying or time-invariant. The focus of this work is on the grey-box, linear, time-invariant (LTI) resistance-capacitance (RC) model identification, which is based on the electrical analogy to model the flow of heat. Several techniques for the determination of the RC parameters for buildings have been investigated in the literature; see [10] for an extensive review of model identification. Typically, the model's output is the building's indoor temperature and inputs comprise of the outdoor ambient temperature, the solar irradiance, and the HVAC output, among others. These signals are usually measured on site and/or available from a nearby weather station.

Unmeasured inputs are termed as disturbances in this work and arise mainly due to varying building occupancy level. These involve the heat energy from the occupants' bodies, lighting and equipment used by the occupants, and can be quite significant and play a determinant role in achieving appropriate temperature control. Most papers in the literature deal with the unmeasured disturbances in one of the following ways: either they are completely neglected or appropriate data is collected in the absence of heat gains due to occupants, or use is made of previous knowledge of occupancy schedule and lighting/equipment details and corresponding assumptions made about the occupant-induced heat gains. Many commercial buildings, even though equipped with Building Management Systems, do not have the capability to measure these thermal gains. Neglecting disturbances generally results in poor model identification [11]. The absence of occupants implies that the building will have to be unused for some time, in order to collect data, and this can be impractical. If a building has a regular operational schedule, such as an office, then assuming the occupancy pattern can be useful. A method to simultaneously estimate the model and the disturbance has the advantage that a model can be trained to forecast the disturbance in predictive control algorithms.

Only a few papers have dealt with the problem of identifying both an RC model and the associated disturbance from data. The technique presented in [11] identifies a disturbance at the output of the model, in order to compensate for the disturbance acting as input to the model. Although not physically meaningful, the

978-1-7281-6746-6/20/$31.00 

result can be useful for predictive control. In [12], [13] and [14], the model was first identified using data collected during unoccupied periods. Data from occupied periods was subsequently used to identify the disturbance. This has the disadvantage that unmodeled dynamics are not captured. A technique called the Simultaneous Plant and Disturbance Identification (SPDI) was proposed in [15] to cater for the previously mentioned deficiencies as applied to a single thermal zone, but the method has not been investigated in the presence of constraints and has not been compared to other existing techniques.

Previous literature review has not shown evidence of any research work dealing with the use of the Extended Kalman Filter (EKF) to simultaneously identify a building thermal model and the disturbance. Moreover, the work in [15] made no mention about the imposed constraints, the initial conditions, the impact of noisy measurements, and the size of the parameter search space. Thus, the aim of this work is to extend the study in [15], and additionally compare the technique to the EKF-based identification.

## II. Methodology

### A. Thermal model

The 2nd order RC thermal model used in this work is shown in Fig. 1.

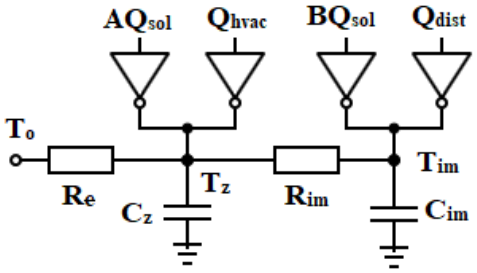


Fig. 1. 2nd order RC model

The parameters are defined as follows: To: Outside air temperature (°C), $T_z$: Measured zone operative temperature (°C), $T_{im}$: Internal mass temperature (°C), A: Factor which decides about the part of the GHI which is convective and has a direct impact on the zone air temperature (36.08 $m^2$), B: Factor which decides about the part of the GHI which is radiative and has a direct impact on the internal mass of the zone (56.31 $m^2$). The internal mass will absorb the energy first, before releasing it to the zone air, $Q_{sol}$: GHI (kW/$m^2$), $Q_{hvac}$: Heating/Cooling power assumed to be convective only, $Q_{dist}$: Disturbances (occupants, equipment and lighting) heat gain, $R_e$: Thermal resistance linking the outdoor air to the zone air (0.429 K/kW), $R_{im}$: Thermal resistance linking the zone air to the internal mass in the zone (0.128 K/kW), $C_{im}$: Thermal capacitance of the internal thermal mass (8.39 x $10^5$ kJ/K), and $C_z$: Zone air thermal capacitance (1.34 x $10^5$ kJ/K). The continuous-time dynamic model is described by equations (1) and (2).

$$C_z\dot{T}_z = \frac{T_o - T_z}{R_e} + \frac{T_{im} - T_z}{R_{im}} + AQ_{sol} + Q_{hvac} \quad (1)$$

$$C_{im}\dot{T}_{im} = \frac{T_z - T_{im}}{R_{im}} + BQ_{sol} + Q_{dist} \quad (2)$$

A continuous time (CT) state space (SS) model of the RC structure can be formulated using the dynamic equations. The only measurement in this model is the state $T_z$. The model can be augmented to include the disturbance as a state to be estimated by a filtering technique. This is possible only if the disturbance is assumed to stay constant over each time step, i.e., it is piecewise constant. To enable the use of sampled input-output data, the CT model was discretized with a sampling time period of 5 minutes, using the zero-order hold technique, to obtain a discrete time (DT) LTI model. The assumed model was simulated with the input data shown in Fig. 2 and an initial state of $[T_z, T_{im}]=[23.5,25]$. The resulting output is also shown in Fig. 2 and was then used alongside the known inputs to identify both the model and the disturbance.

### B. SPDI algorithm

Readers are referred to [15] for a detailed description of the algorithm, which involves the application of a linear Kalman filter (KF) inside an optimization algorithm for the determination of the R and C parameters as well as the disturbance. A summary of the steps is presented as follows:

1. Define the R and C parameter search space
2. Select an initial parameter vector using Latin Hypercube Sampling (LHS)
3. Use the vector to compute the DT SS matrices of the augmented SS model
4. Use a linear KF to estimate the state and then compute the objective function of the optimization
5. Based on the objective function, the parameter vector is updated and steps 1-5 repeated until some stopping criterion is reached
6. Save the optimum parameter vector

The objective function to be minimized in this work was the sum of squared error (SSE) between the estimated and actual zone temperatures over a certain number of time samples. Given that the objective was a non-convex function of the parameter vector, the optimization could lead to a local minimum, depending on the initial parameter guess. Therefore, steps 1-5 were solved for 30 times, each time starting with a distinct initial guess provided by LHS. At the end, 30 optimal solutions were obtained, and the median solution was calculated to be the identified parameter vector, compared to the mode employed in [15]. The identified parameters were then used to estimate the disturbance. Data for the first 20 days (5760 points) were used to identify the model and the disturbance. The parameter search space was defined to be in a narrow range of 0.7 $x$ to 1.3 $x$, where $x$ is the nominal parameter value provided in part A. For the KF, the process and measurement error covariances Q and R respectively were selected to be time invariant as provided in Table I. No noise or very little noise was assumed to be present in the measurement data. The covariances will guide the KF to trust the measurements more than the modelling. The error covariance (EC) matrix was selected as shown in Table I to represent the confidence in the initial state guess. $T_{im}$ is not a measured quantity, so that its covariance is relatively high, to consider a maximum possible error of 5°C in the assumed initial temperature.

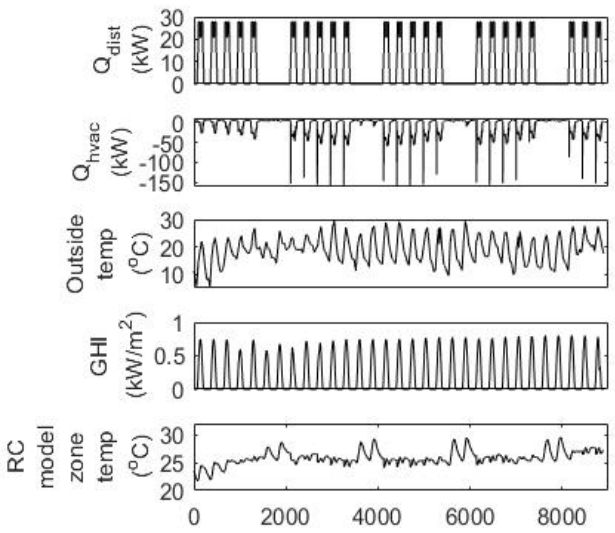


Fig. 2. Model input signals

For $T_z$, the covariance is low, given that it is a known parameter. $Q_{dist}$ can erroneously be assumed to be 0 initially, when it is actually equal to the maximum value of 27.75 kW, or vice versa. Thus, a maximum error of about 30 kW has been considered.

No constraints on the estimated states were considered in [15]. In this work, linear inequality constraints were imposed on the estimated states as shown in Table I. The constraints were considered only while using the final identified parameter vector to estimate the disturbance, as their incorporation in every KF step of the SPDI would make the latter take a much longer time to run. More details about imposing constraints are provided in [16].

To study the impact of noisy measurements, random noise with reasonable standard deviations were added to the input-output data. The standard deviations were 0.15 $^oC$, 0.025 $kW/m^2$, 0.25 kW and 0.2 kW for the temperatures, GHI, $Q_{hvac}$ and $Q_{dist}$ respectively. The noisy GHI and $Q_{dist}$ data were not allowed to contain negative values. To study the impact of the initial state on the estimation, $T_{im}$ was assumed to be 20$^o$C in 1 case and 30$^o$C in another case, rather than the correct value of 25$^o$C. To investigate the impact of the size of the parameter search space, wide parameter bounds were imposed on the parameters as follows: All parameters had a minimum value of 0. A and B had maximum values of 160. $R_e$ and $R_{im}$ had maximum values of 100 K/kW. $C_z$ and $C_{im}$ had maximum values of 5 x $10^6$ kJ/K.

### *C. EKF algorithm*

The simultaneous estimation of the states and parameters is referred to as joint-estimation. Details about the equations are provided in [12]. Even if the model is linear, augmenting the state vector with the parameters yields a non-linear problem. Therefore, the non-linear KF, EKF, was used to estimate the RC parameters as well as the disturbance. For the EKF, the process error covariance (PEC) matrix for the corresponding augmented state vector is shown in Table I. The measurement error covariance (MEC) and the EC matrix are also provided in Table I. The very low PEC of $10^{-20}$ for the parameters represent the time-invariability of the parameters. The PEC for the temperature and disturbance states are the same as for the SPDI. The MEC is the same as for the SPDI. The EC for the temperature and disturbance states is the same as for the SPDI. The EC for the parameters were calculated based on the estimate of the maximum error in the initial guess. The temperature and disturbance state constraints were the same as for the SPDI. The constraints for the parameter states were the same as the narrow range boundaries used for the SPDI. Given that the convergence for the EKF takes some time, the root mean square error (RMSE) of the disturbance was calculated over 1000 data points only (4761 to 5760) for both the SPDI and the EKF. Moreover, the EKF-converged parameters were calculated as the average of their values over the last 1000 iterations (4761 to 5760 data points) only.

Table I. Algorithm parameters

| **Parameters** | **KF in SPDI** | **EKF** |
|---|---|---|
| Q | diag ($10^{-4}$, $10^{-4}$, $10^3$) | diag ($10^{-4}$, $10^{-4}$, $10^{-20}$, $10^{-20}$, $10^{-20}$, $10^{-20}$, $10^{-20}$, $10^{-20}$, $10^3$) |
| R | $10^{-8}$ | $10^{-8}$ |
| EC | diag (1, 25, 1000) | diag (1, 25, 0.02, 2 x $10^9$, 0.0015, 6.5 x $10^{10}$, 150, 300, 1000) |
| Augmented State Vector | x = ($T_z$, $T_{im}$, $Q_{dist}$) | x= ($T_z$, $T_{im}$, $R_e$, $C_z$, $R_{im}$, $C_{im}$, A, B, $Q_{dist}$) |
| Initial state (IS) | SSE1 = [23.5, 25] | IS1 = [23.5, 25] |
| | SSE2 = [23.5, 20] | IS2 = [23.5, 20] |
| | SSE3 = [23.5, 30] | IS3 = [23.5, 30] |
| Constraints | $20 \leq T_z \leq 30$<br>$20 \leq T_{im} \leq 30$<br>$0 \leq Q_{dist} \leq 27.75$ | $20 \leq T_z \leq 30$<br>$20 \leq T_{im} \leq 30$<br>$0 \leq Q_{dist} \leq 27.75$<br>$0.300 \leq R_e \leq 0.558$<br>$0.0896 \leq R_{im} \leq 0.166$<br>$9.38 \times 10^4 \leq C_z \leq 1.74 \times 10^5$<br>$5.87 \times 10^5 \leq C_{im} \leq 1.09 \times 10^6$<br>$25.26 \leq A \leq 46.90$<br>$39.42 \leq B \leq 73.20$ |

## III. RESULTS AND DISCUSSIONS

The RMSE in the estimated disturbance for the 30 initial parameter vector guesses (IPGs) is shown in Fig. 3 for the unconstrained case and in Fig. 4 for the constrained case. The initial state information for SSE1, SSE2, SSE3, IS1, IS2 and IS3 are provided in Table I. For the different IPGs, EKF generally performs better than SPDI both in the presence and absence of constraints, as depicted by a lower RMSE disturbance. The constraints in the SPDI algorithm decrease the RMSE of the estimated disturbance significantly. The initial state guess (ISG) does have an impact on the RMSE disturbance as per Fig. 3 and Fig. 4, depending on the IPG. For EKF, IS1 provides a lower RMSE disturbance most of the time. The parameters estimated

over the 30 IPGs are much more scattered (box plots of the parameters are not shown here due to space limitations) for the SPDI rather than for the EKF, due to local minima resulting in the former. Fig. 5 and Fig. 6 show the SPDI-estimated disturbance for SSE 1 when using the median parameter vector, without constraints, and with constraints respectively. The constraints keep the estimated disturbance bounded. The RMSEs in the estimated disturbance are 4.81 kW and 4.58 kW respectively. The RMSEs in the simulated zone temperatures using the estimated disturbance are 0.024 ºC and 0.029 ºC for the unconstrained and constrained conditions respectively. When the median parameter vector is used to estimate the disturbance, constraints do not bring much improvements. Moreover, the RMSE disturbance using the median parameters were not significantly different for the SSE1, SSE2 and SSE3 ISGs. Fig. 7 and Fig. 8 show the disturbances estimated using EKF under unconstrained and constrained conditions respectively, for IS1 and for the IPG which produced the minimum disturbance RMSE (Initial guess 17 in Fig. 3).

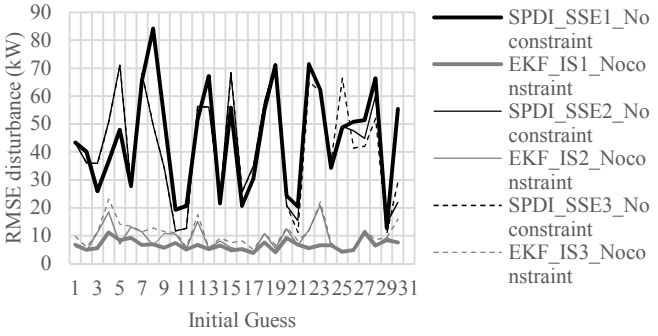


Fig. 3. RMSE of estimated disturbance (kW)-Unconstrained

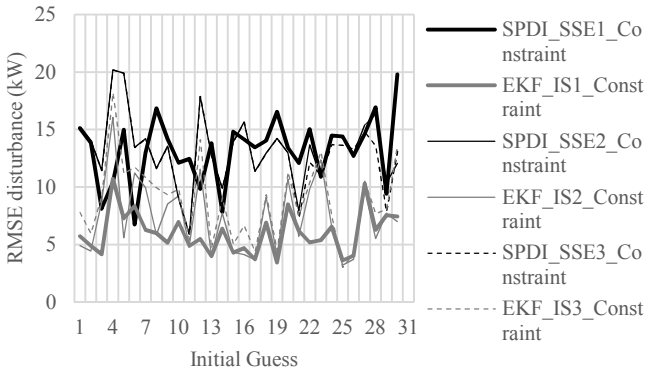


Fig. 4. RMSE of estimated disturbance (kW)-Constrained

The RMSEs in the estimated disturbance are 3.88 kW and 3.73 kW respectively. The RMSEs in the corresponding simulated zone temperatures using the estimated disturbance are 0.029 ºC and 0.033ºC for the unconstrained and constrained conditions respectively. The addition of constraints do not provide significantly better results after convergence of states have been achieved. Therefore, it can be deduced that the EKF can produce nearly the same results as the SPDI, but at much lower computational expense. The unconstrained EKF algorithm for all the 30 guesses ran over 48 seconds, while the SPDI algorithm, with constraints considered only for the median parameters ran over 1678 seconds. The constrained EKF algorithm ran over 880 seconds, while the SPDI algorithm with constraints considered for each IPG had not yet completed after 3 hours of run.

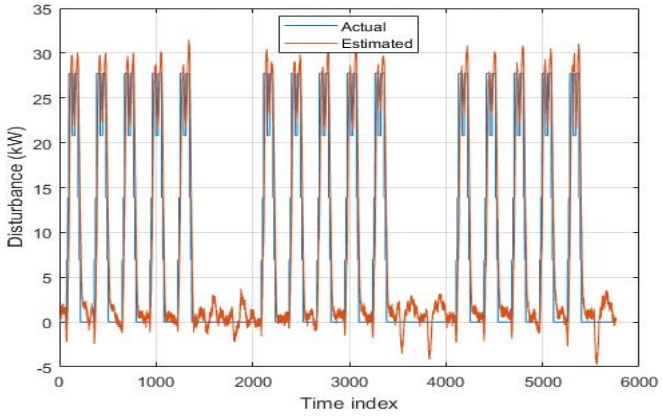


Fig. 5. SPDI Estimated disturbance - Unconstrained

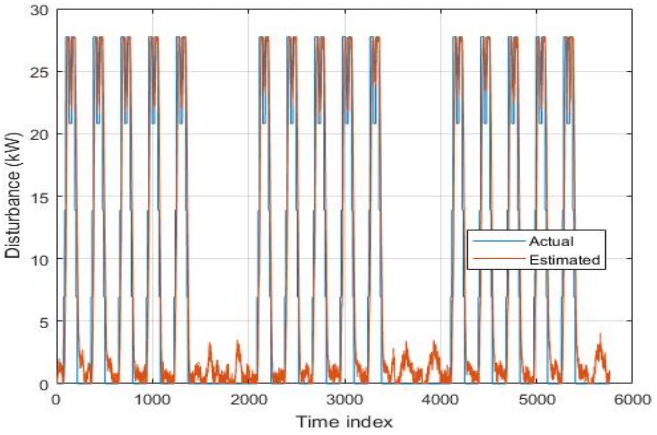


Fig. 6. SPDI Estimated disturbance - Constrained

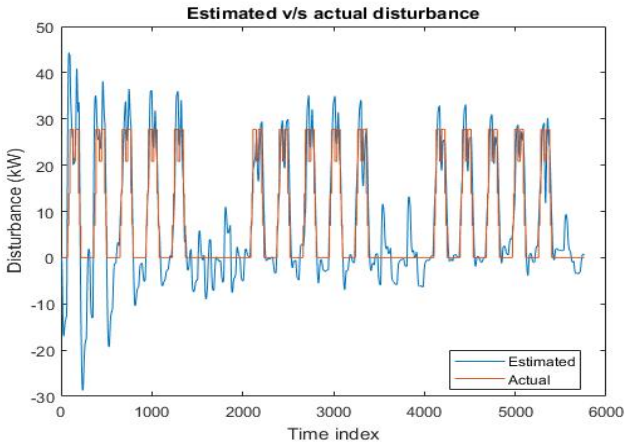


Fig. 7. EKF Estimated disturbance - Unconstrained

One drawback with the EKF is that a minimum number of data points is needed to allow for the state convergence to occur as shown in Fig. 9, and this issue does not arise with the SPDI, which works by simply trying to 'fit' the model response to the

actual measurement. The results for the wide parameter range and noisy conditions could not be included due to space requirements. Both the SPDI and EKF show poor performance in the presence of noisy signals or when the parameter search space is wide.

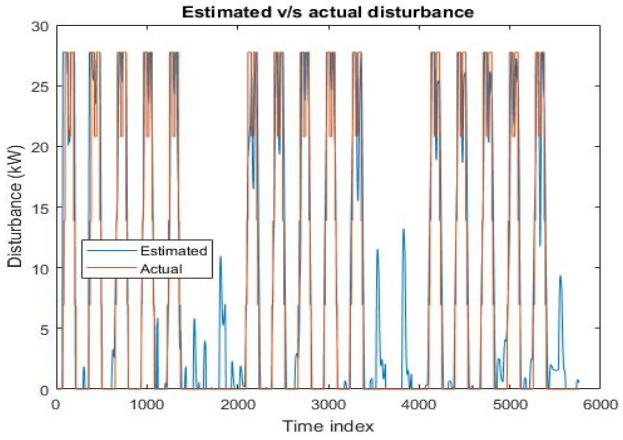


Fig. 8. EKF Estimated disturbance – Constrained

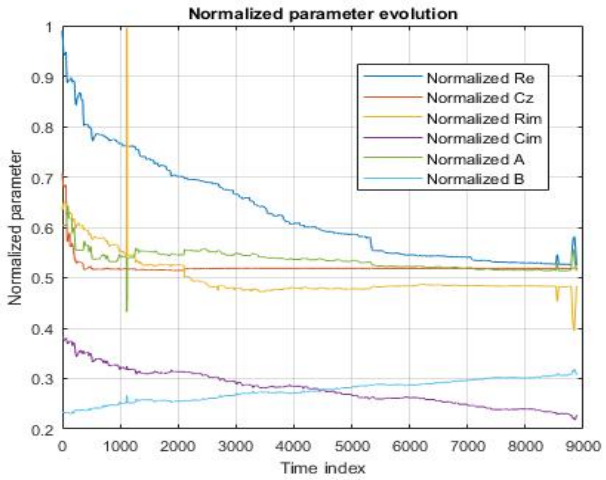


Fig. 9. Normalized parameter evolution for constrained EKF for initial guess 17

## IV. Conclusion

In this work, a comparison of an EKF-based and an optimization based approach is made in an effort to determine their efficiency and accuracy to simultaneously identify a building thermal zone 2nd order RC grey-box model and estimate the unknown disturbance. It was found that the optimization algorithm is more computationally expensive than the EKF, while producing similar results. The optimization technique may become better when insufficient identification data is available, given that the EKF needs a minimum amount of data for convergence to be complete. Both algorithms are not able to cope well with wide parameter ranges and noisy data. The initial guess of the states was found to have an impact on the disturbance estimation results. Constraints introduced in the algorithms do not seem to bring much improvement in the final estimated disturbances. However, when the disturbances are estimated using parameters resulting from local optimum in the SPDI algorithm, the constraints tend to bring significant improvements. Future work will involve more detailed analyses on closed loop identification data as well as the effect of data quality on the estimates.

## References

[1] IEA, "IEA the critical role of buildings," 2019. [Online]. Available: https://www.iea.org/reports/the-critical-role-of-buildings. [Accessed: 05-Apr-2020].

[2] D. Ürge-Vorsatz, L. F. Cabeza, S. Serrano, C. Barreneche, and K. Petrichenko, "Heating and cooling energy trends and drivers in buildings," *Renewable and Sustainable Energy Reviews*, vol. 41. Elsevier Ltd, pp. 85–98, 01-Jan-2015.

[3] S. Salakij, N. Yu, S. Paolucci, and P. Antsaklis, "Model-Based Predictive Control for building energy management. I: Energy modeling and optimal control," *Energy Build.*, vol. 133, pp. 345–358, 2016.

[4] W. Kim and S. Katipamula, "A review of fault detection and diagnostics methods for building systems," *Sci. Technol. Built Environ.*, vol. 24, no. 1, pp. 3–21, Jan. 2018.

[5] J. Vivian, A. Zarrella, G. Emmi, and M. De Carli, "An evaluation of the suitability of lumped-capacitance models in calculating energy needs and thermal behaviour of buildings," *Energy Build.*, vol. 150, pp. 447–465, 2017.

[6] R. De Coninck and L. Helsen, "Practical implementation and evaluation of model predictive control for an office building in Brussels," *Energy Build.*, vol. 111, pp. 290–298, Jan. 2016.

[7] A. Afram and F. Janabi-Sharifi, "Review of modeling methods for HVAC systems," *Appl. Therm. Eng.*, vol. 67, no. 1–2, pp. 507–519, 2014.

[8] A. Martincevic and M. Vasak, "Constrained Kalman Filter for Identification of Semiphysical Building Thermal Models," *IEEE Trans. Control Syst. Technol.*, vol. PP, pp. 1–8, 2019.

[9] E. Atam and L. Helsen, "Control-Oriented Thermal Modeling of Multizone Buildings: Methods and Issues: Intelligent Control of a Building System," *IEEE Control Syst.*, vol. 36, no. 3, pp. 86–111, 2016.

[10] Z. Wang and Y. Chen, "Data-driven modeling of building thermal dynamics: Methodology and state of the art," *Energy Build.*, vol. 203, 2019.

[11] D. Kim, J. Cai, K. B. Ariyur, and J. E. Braun, "System identification for building thermal systems under the presence of unmeasured disturbances in closed loop operation: Lumped disturbance modeling approach," *Build. Environ.*, vol. 107, pp. 169–180, 2016.

[12] S. F. Fux, A. Ashouri, M. J. Benz, and L. Guzzella, "EKF based self-adaptive thermal model for a passive house," *Energy Build.*, vol. 68, no. PART C, pp. 811–817, 2014.

[13] Q. Hu, F. Oldewurtel, M. Balandat, E. Vrettos, D. Zhou, and C. J. Tomlin, "Building model identification during regular operation," pp. 1–6, 2016.

[14] P. Radecki and B. Hencey, "Online building thermal parameter estimation via Unscented Kalman Filtering," in *Proceedings of the American Control Conference*, 2012, pp. 3056–3062.

[15] A. R. Coffman and P. Barooah, "Simultaneous identification of dynamic model and occupant-induced disturbance for commercial buildings," *Build. Environ.*, vol. 128, pp. 153–160, 2018.

[16] G. Lillacci and M. Khammash, "Parameter estimation and model selection in computational biology," *PLoS Comput. Biol.*, vol. 6, no. 3, 2010.